Prevention of colorectal cancer liver metastasis by exploiting liver immunity via chitosan-TPP/nanoparticles formulated with IL-12

Qiongming Xu [a,1], Lingchuan Guo [b,1], Xinhua Gu [c], Biao Zhang [b], Xin Hu [b], Jiajia Zhang [b], Jinghong Chen [b], Yi Wang [b], Cheng Chen [b], Bei Gao [b], Yuting Kuang [d,**], Shouli Wang [b,*]

[a] Department of Pharmaceutical Chemistry, Soochow University College of Pharmaceutical Science, Suzhou 215123, China
[b] Department of Pathology, Soochow University School of Medicine, Suzhou 215123, China
[c] Department of Surgery, Suzhou City Hospital, Suzhou 215008, China
[d] Department of Surgery, First Affiliated Hospital, Soochow University, Suzhou 215006, China

ARTICLE INFO

ABSTRACT

The development of effective therapies for the prevention of colorectal cancer (CRC) liver metastasis is of great importance. Recently, chitosan (CS) nanoparticles have been utilized as carriers of interluekin-12 (IL-12) administered locally to deliver therapeutic proteins and genes. In this study, we encapsulated IL-12 by incorporation using tripolyphosphate (TPP) as the coacervated crosslinking agent to form CS-TPP/IL-12 nanoparticles. We further characterized the association efficiency, rate of release, liver-targeting, and toxicity, which were predominantly dependent on the factors of particle size, zeta potential, pH of solution, and whether or not modified with TPP. Systemic delivery of CS-TPP/IL-12 nanoparticles significantly reduced the number and volume of CRC liver metastasis foci compared to the CS-TPP treated mouse group. Although delivery of IL-12 alone also inhibited the number of CRC liver metastasis observed, further study of the change in hepatic metastasis volume demonstrated no significant differences between the groups treated with CS-TPP or IL-12 alone. Mechanistically, CS-TPP nanoparticles blocked the toxicity of IL-12 and induced infiltration of NK cells and some T cells, which are most likely the effector cells that mediate tumor metastasis inhibition during CS-TPP/IL-12 immunotherapy. The results obtained from this study demonstrate the potential benefit of using chitosan modification technology as a cytokine delivery system for the successful prevention of CRC liver metastasis by exploiting liver immunity.

© 2012 Elsevier Ltd. All rights reserved.

1. Introduction

Colorectal cancer (CRC) is frequently complicated by the occurrence of metastatic disease, which most commonly presents in the liver and is responsible for approximately 70% of CRC-related deaths [1]. The present management of CRC liver metastasis that includes surgical resection, combination chemotherapy, and biological therapy is frequently palliative [2] and increasing evidence has emerged indicating that surgery paradoxically enhances metastasis development [3–5], and the various systemic agents and regiments commonly utilized are associated with a wide spectrum of toxic effects [6,7]. Therefore, identification of new biological markers to help determine the patients most likely to

respond to a newer agent is a current trend in CRC liver metastasis management [2]. In fact, because CRC liver metastasis is the result of an imbalance between the immunological escape of CRC cells and the immune surveillance system of the liver [8,9], and as it has been demonstrated that the growth of metastatic CRC cells is under the control of an immunotherapy that relies on the contribution of the host immune system [10,11], exploitation of liver resident immunity to control CRC liver metastasis is warranted [12].

Interleukin-12 (IL-12) is a multifunctional cytokine that enhances T helper cell 1 (Th1) differentiation, cellular immunity, proliferation of natural killer and activated T cells [13], and has been demonstrated to be one of the most effective inducers of potent antitumor immunity [13,14]. Unfortunately, excessive toxicity following administration of intravenous IL-12 has proven to be a major obstacle to its clinical application [15–17]. Although researchers have developed virus-based and gene-modified cell-based IL-12 therapies with decreased toxicity [18,19], the generation of neutralizing antibodies is a limitation to this mode of administration [18]. Currently, nonviral delivery approaches for

IL-12 protein or gene expression vectors are being defined, including liposomes, polymers, lipids, and alum-based delivery systems [16]. Among various nonviral vectors, chitosan (CS) is a suitable candidate for macromolecular delivery [20,21]. Recently, local administration to the orthotopic bladder tumor of either CS-based nanoparticle delivery plasmids encoding murine IL-12 or IL-12 cytokine in mice bearing CT-26 carcinoma cells [22] has been demonstrated [23]. In theory, local administration carries the advantage of the preferred paracrine mechanisms of cytokine action and reduces systemic toxicity; however, the requirement of an accessible site for administration has limited the potential for wide-spread use in cancer therapy. Since the passive liver-targeting characteristic of the microparticles after i.v. administration is dependent on particle diameter and physico-chemical property [24,25], the ability to modulate these properties is central in determining liver-targeting efficiency of nanoparticles. Thus, in this study we hypothesized that modification of CS with ionic gelation of tripolyphosphate (TPP) would not only generally increase the capacity for association of macromolecules as previously described [20], but also improve IL-12 loaded nanoparticle distribution in the liver. We systematically manipulated the processing parameters during TPP initiated CS gelation to obtain optimal IL-12 nano-carriers that maintain stability during circulation and subsequently transform to the IL-12- releasing form by Kupffer cells directed toward lysosomes, where they digested by lysosomal acid hydro-lases. Finally, we investigated the liver immune microenvironment in an effort to elucidate the mechanisms by which CS-TPP/IL-12 nanoparticles stimulate immune activity in the liver.

2. Materials and methods

2.1. Cell culture

CT26 murine colon carcinoma cells, syngeneic to Balb/c mice, were obtained from American Type Culture Collection (Manassas,VA). CT26 cells were grown as monolayer cultures in DMEM with 10% FBS (Invitrogen, Carlsbad, CA) supplemented with 100 IU/ml Penicillin and 100 mg/ml Streptomycin. Cells were maintained in a 37 °C incubator with 5% CO_2 humidified air.

2.2. Preparation and measurement of particle size and zeta potential of CS-TPP/IL-12 nanoparticles

Chitosan glutamate, with a molecular weight of 470 kDa and degree of deacety-lation of 86% (granted by Xingcheng Biological Industrial Limited Co. Nantong, China), was dissolved in an acetic acid solution. Pentasodium tripolyphosphate (TPP) was obtained from Sigma–Aldrich (St. Louis, MO). Chitosan nanoparticles were created by modified ionic gelation with negatively charged TPP ions, as reported in our previous studies [20] and other studies [26]. The weight ratio of chitosan to TPP (CS-TPP ratio) ranged from 2/1 to 14/1. The recombinant murine IL-12 (R&D Systems, Abingdon, UK)–loaded nanoparticles were formed as follows: IL-12 was dissolved in PBS at various concentrations (0.5, 1, 1.5 and 2 µg/mL), next 1 mL IL-12 solution was added to the chitosan solution (3 mL, 2 mg/mL) prior to the incorporation of the TPP solution (1.2 mL, 0.84 mg/mL). The particles were incubated for 30 min at room temperature before use or further analysis. The physical size and zeta potential of the nanoparticles were measured using a 3000HSA Zetasizer (Malvern Instruments, England).The morphology of nanoparticles was observed by scanning electron microscopy (SEM).

2.3. Monitoring in-vivo characteristics of CS-TPP/IL-12 nanoparticles in tumor-bearing mice

All procedures involving animals were approved by our current institutional regulations for use and care of laboratory animals. Balb/c mice (6−8 weeks of age) were obtained from SLAC Laboratory Animal Co. Ltd (Shanghai, China). To determine the biodistribution of CS-TPP/IL-12 nanoparticles, we evaluated fluorescence iso-thiocyanate (FITC)-labeled CS-TPP or CS alone by chemical bond. Briefly, a CS acetic acid solution, along with an alcohol solution containing FITC, was exposed to magnetic-driving conditions. The mixture was then stored in a cool, dark place for 4 h; subsequently, the pH of the mixture was regulated with 10 M NaOH followed by centrifugation and washed with distilled water. Next, the precipitate was dissolved with 2% acetic acid solution and the pH of the mixture was regulated to a pH of six. Lastly, the mixture, along with a TPP solution, was exposed to conditions of magnetic-driving for 20 min, and the final result was FITC labeled CS-TPP nano-particles (FITC–CS-TPP). The biodistribution of FITC–CS-TPP nanoparticles in tumor-

bearing mice (see later in section of 2.6) was determined according to the fluores-cence intensity (FI) of each tissue following a tail injection. Mice were injected with 0.2 ml of a range in size of FITC-nanoparticles or nanoparticles either modified with TPP or not modified. Animals were sacrificed at 4, 24, and 48 h following injection, organ homogenates were prepared, and FI of supernatant preparations were analyzed with an F-4000 fluorescence spectrometer (HITACHI, Japan). Liver frozen sections were prepared and photographed under a fluorescence microscope (BX2-FLB3-000; OLYMPUS, Japan). The measured FI of organs was corrected according to the weight of tissue. The FI was calculated as follows: FI = (Fs − Fb)/Fs × 100%, where Fs is the FI of the sample, Fb is the FI of blank control and Fs is the FI of the standard. The experiment was performed at least three times per experimental group.

2.4. Toxicity and pathology

To measure plasma cytokine levels of mice above, blood was harvested from the animals 1, 3, 6, and 12 days after daily intravenous injections with 0.5 µg recombi-nant murine IL-12 alone or loaded in CS or CS-TPP nanoparticles. The blood was harvested from mice via cardiac puncture and plasma was isolated using Micro-tainer tubes (BD) to analyze liver enzymes such as alanine aminotransferase (ALT), aspartate aminotransferase (AST), and cytokine IFN-γ. IFN-γ levels were measured by enzyme linked immunosorbent assay (ELISA) according to the manufacturer's instructions (Jingmei Biotech, China). The major organs of the mice were collected, formalin fixed, and processed for routine H&E staining using standard methods.

2.5. Determination of IL-12 association efficiency and release of IL-12 in-vitro

The association efficiency (AE) of IL-12 in CS-TPP nanoparticles was obtained by determination of the unbound IL-12 concentration in the supernatant recovered after particle centrifugation (20,000 × g, 20 min). The free IL-12 in the supernatant was determined using ELISA kits (Jingmei Biotech, China) and compared to the total IL-12 initially added. The AE of IL-12 was calculated using the formula: AE = ([Total amount of IL-12] − [IL-12 in supernatant])/Total amount of IL-12 × 100%. To measure the release of IL-12, the formulated nanoparticles were centrifuged at 8000 × g for 20 min, and each weighed pellet was reconstituted with three mL of dissolution medium under agitation. The acetic acid solution pH ranged from 5 to 7. The amount of IL-12 released was expressed as a percentage of the total IL-12 loaded with the nanoparticles as described above.

2.6. Antitumor efficacy of CS-TPP/IL-12 nanoparticles in CRC hepatic metastasis model

To select the optimal murine hepatic metastasis model of CRC, Balb/c mice were grouped randomly into three groups, with injections of 0.2 mL CT26 cells (1 × 10⁶/ mL) via rectum transplant, peritoneal cavity spleen transplant and intraperitoneal spleen transplant. The number of hepatic metastasis was counted and level of INF-γ was detected by ELISA after five days. Because the INF-γ level was considered one of the most sensitive cytokines following surgical operation [27,28], INF-γ was examined by ELISA to evaluate the degree of injury. Two weeks after establishment of the CRC liver metastasis model, each mouse was injected daily with 0.1 µg or 0.2 µg of recombinant murine IL-12 loaded in CS-TPP, or 0.2 µg IL-12 alone as a control. The mice were sacrificed 21 days after tumor treatment challenge, the number of hepatic metastases was counted, and the tumor volumes were calcu-lated as a $\times$ b²/2, in which a represents the largest and b the smallest diameter. In order to precise comparison of metastasis tumor size, the liver weight in each group was used to standardization.

2.7. Western blot analysis, release of IL-12 in-vivo

We explored the release of IL-12 in-vivo utilizing Western blot analysis of IL-12 in liver tumor tissue of mice treated with nanoparticles containing IL-12 and CS-TPP alone (as mentioned above). In brief, liver tumor tissue was harvested and lysed in TNES buffer and equal amounts of total protein were electrophoresed on 8% SDS polyacrylamide gels and electrotransferred onto polyvinyl difluoride membranes. The membranes were blocked with 1 × TBS that contained 5% nonfat powdered milk (w/v), 0.02% sodium azide, and 0.02% Tween-20, and incubated with IL-12 mono-clonal antibody (Santa Cruz Biotechnology, Santa Cruz, CA, USA), diluted at 1:1000. After washing, primary antibodies were detected with peroxidase-conjugated secondary antibodies, diluted at 1:2000 using an enhanced chemiluminescence detection system. Equal sample loading was demonstrated by anti-β-actin immu-noblotting (Santa Cruz Biotechnology).

2.8. Immunohistochemical and immunofluorescence staining

Livers were removed and fixed in 10% neutral buffered formalin. Sections of paraffin-embedded tumor tissue (4.0 µm thick) were incubated with 0.3% hydrogen peroxide (H_2O_2) in methanol for 30 min to block endogenous peroxidase activity. Next, the slides were exposed to rabbit anti- CD8 (DAKO, Denmark) for 30 min and incubated for 20 min with biotinylated anti-immunoglobulins and then incubated for 20 min with biotinylated peroxidase–streptavidin complex. The sections were

then stained for 5 min with 3, 3′-diaminobenzidine (DAB) freshly prepared in 0.05 M Tris−HCl buffer at pH7.6. After counterstaining with hematoxylin, the sections were dehydrated and mounted. To determine whether CD4+ T cells were involved in tumor-infiltration, sections were blocked with 5% goat serum in PBS that contained 1% BSA at 37 °C for 30 min. Then, sections were incubated at 4 °C overnight with anti- CD4 (DAKO, Denmark) in PBS containing 1% BSA. After the cells were washed with PBS, a 1:100 dilution of FITC-conjugated IgG was applied as the secondary antibody for 1 h at room temperature. The slides were washed, mounted, and photographed under a fluorescence microscope (BX2-FLB3-000; Olympus).

2.9. Isolation of mononuclear cells from liver and from the cytotoxicity assay

The livers were homogenized, passed through a 70 μm cell strainer (BD Biosciences, Mississauga, ON, Canada), and washed in HBSS containing 1%FBS (wash solution). After an additional wash, the cell pellet was resuspended in 5 ml of wash solution, underlayed with 5 ml of lymphocyte-M solution (Cedarlane, Ontario, Canada), and centrifuged at 1,000 g for 25 min and mononuclear cells (MNCs) were collected and washed before further use. The NK assay was performed with freshly isolated MNCs from livers at 2, 4, 8, and 16 (6 mice/group/time point) days after treatment. The effectors were incubated with ^{51}Cr-labeled CT26 targets for 4 h at 37 °C at ratios of 100:1. The radioactivity released in the supernatant was measured by a gamma counter and was calculated as follows: (experimental release − spontaneous release)/(maximal release − spontaneous release) × %. We used Thy-1,2 and

PK136 hybridoma supernatant (ATCC) for depletion of T and NK cells, respectively, under established conditions [29]. In brief, MNCs isolated from CS-TPP/IL-12 treated animal livers at day 3 were incubated with the proper concentration of antibody and depleted with complement at 37 °C. Optimal concentrations of antibodies and complement were used and verified by flow cytometry.

2.10. Statistics

The data were presented in the form of mean and standard deviation. The statistical significance of the differences between the experimental and control groups was determined using Student's t-test (2-tailed), with P values <0.05 or <0.01 were considered to represent a significant result. (SPSS 10.0, SPSS Inc., Chicago, IL, USA).

3. Results

3.1. Size and surface charge of CS-TPP/IL-12 nanoparticles

In order to prepare nanoparticles capable of degradability and prolonged circulation, we modified chitosan with TPP (Fig. 1a) and examined the properties. Fig. 1b shows that the mean diameter of the nanoparticles ranges from 178 to 372 nm along with an increase
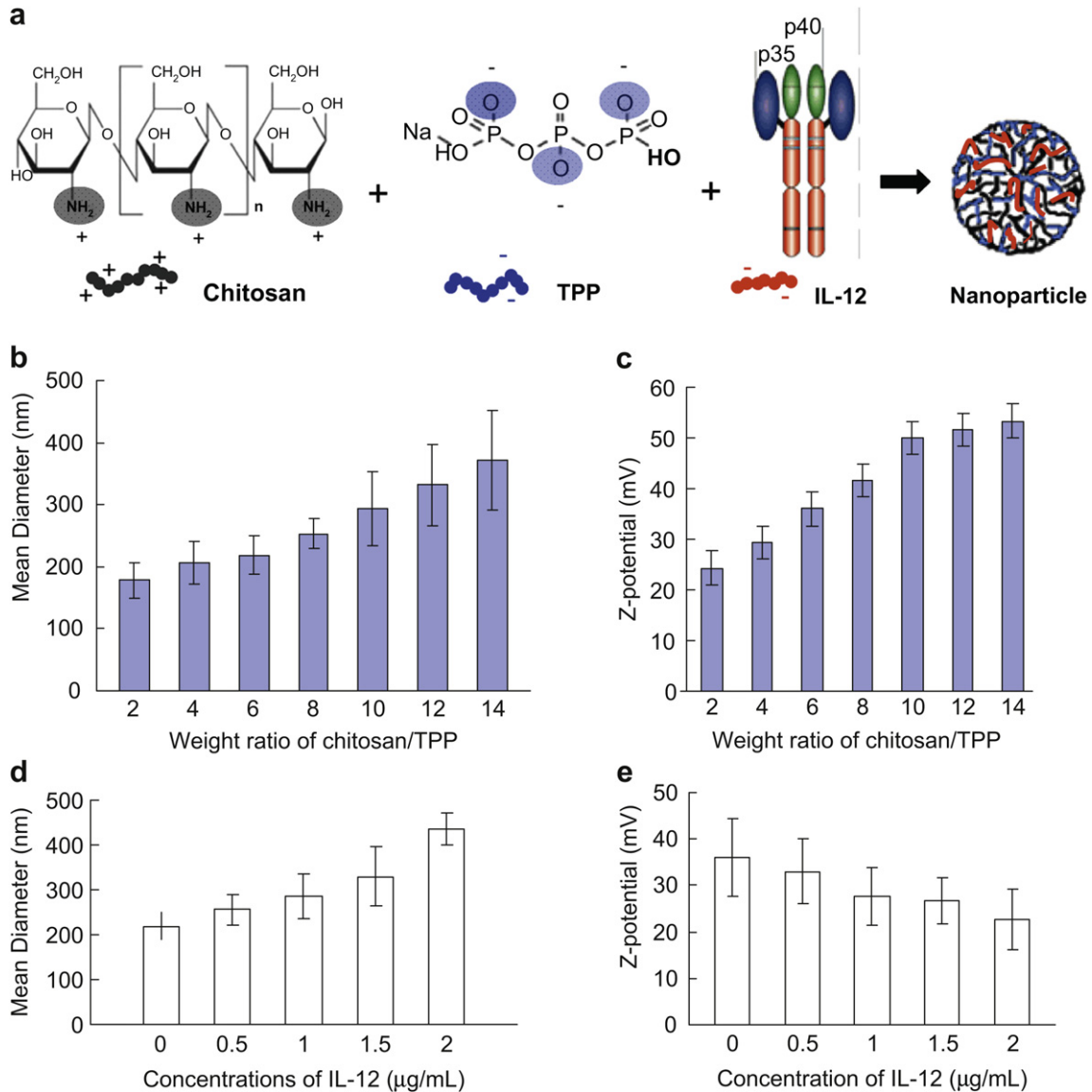
Fig. 1. Synthesis and characteristics of CS-TPP/IL-12 nanoparticle system. (a) Schematic of the proposed approach. (b) Effect of weight ratio from 2:1 to 14:1 on particle size. (c) Effect of weight ratio from 2:1 to 14:1 on zeta potential. (d) Effect of concentration of IL-12 (μg/mL) from 0 to 2 on particle size. (e) Effect of concentration of IL-12 (μg/mL) from 0 to 2 on zeta potential. T = 20 ± 1 °C, pH 7.0.

in the chitosan/TPP weight ratio. Fig. 1c shows that the zeta potential of the nanoparticles ranges from 24 to 53 mV depending on the weight ratio of chitosan to TPP, suggesting a net positive surface charge due to excess chitosan. We next examined the concentrations of IL-12 of effective size and zeta potential of the nanoparticles formulated chitosan to TPP weight ratio 6:1. The incorporation of IL-12 at an increasing concentration led to the formation of larger nanoparticles (Fig. 1d) and a lower zeta potential (Fig. 1e).
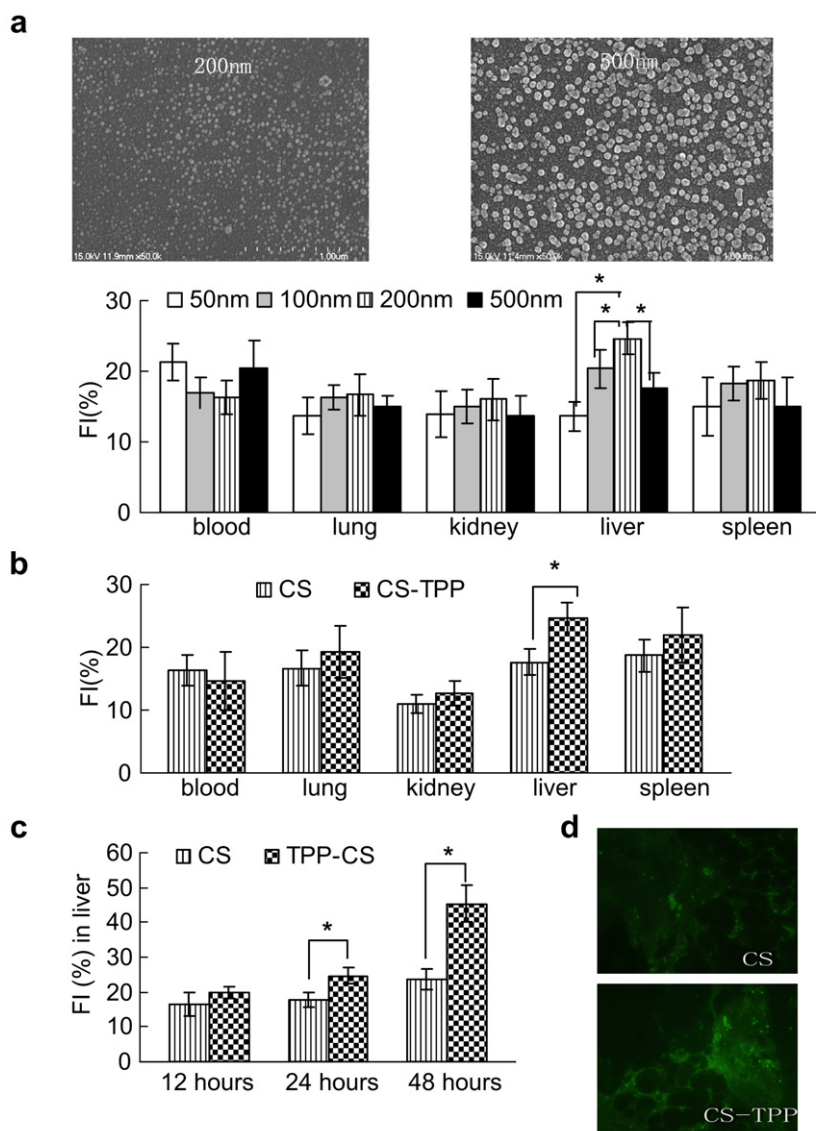
3.2. Particle size and biodistribution of CS nanoparticles

The efficiency of delivery of IL-12 into the liver with different particle sizes (Fig. 2a) and TPP modification or not (Fig. 2b − d) was monitored using FITC-conjugated nanoparticles. FI was examined on major organs homogenates over the span of 24 h following injection. The FI was present at different intensities in organs in association with the different nanoparticle sizes. A lower FI in blood was observed in animals treated with particle sizes ranging from 100 nm

to 200 nm and a higher intensity was found in the mouse groups treated with particle sizes above or below the range. However, a relatively higher FI was observed in the lung, kidney, liver, and spleen in animals treated with particle sizes of 100 nm or 200 nm, particularly in the liver. Therefore, we selected CS-TPP nanoparticle size at 200 nm for further study. Fig. 2b shows that the FI intensity in the organ sections for CS-TPP treated animals is greater compared to FITC-chitosan treated animals. The accumulation of nanoparticles in these organs, which contain the reticuloendothelial system (RES), may be due to phagocytosis [30]. Fig. 2c shows that 12, 24, and 48 h following injection of nanoparticles modified with TPP, the FI was 20%, 24.7%, and 45.3% in the liver, adding to the accumulation of evidence that FITC-CS acts in a time dependent manner.

3.3. CS-TPP shielded toxicity of circulating IL-12 in mice

Comparisons between the IL-12 treated group and the groups treated with CS/IL-12 or CS-TPP/IL-12 reveal that there is

Fig. 2. Effect of preparation conditions on biodistribution of FITC-labeled CS nanoparticles. (a) Representative shapes of CS-TPP via SEM (Scale = 1um) and biodistribution of different sizes of FITC-labeled nanoparticles over 24 h post injection; (b) Biodistribution of FITC-labeled nanoparticles (200 nm) modified with TPP or not 24 h post injection; (c) Liver-targeting of nanoparticles (200 nm) modified with TPP or not at different times post injection; (d) Representative fluorescence images of liver sections bearing CT26 colon cancer metastasis, the mice were sacrificed 2 days after intravenous injection with either FITC-labeled CS or CS-TPP (200 nm) (× 50).

a significant change in level of IFN-γ. As shown in Fig. 3a, the higher level of IFN-γ was observed six days after IL-12 treatment compared to that of the other two groups. Twelve days after treatment with IL-12, the level of IFN-γ decreased gradually; however, the level of IFN-γ in mice treated with CS-TPP/IL-12 persisted and increased, even after 12 days. These results indicated that CS-TPP prolonged the biological function of IL-12 in circulation by increasing level of IFN-γ. The liver enzymes of mice treated with CS-TPP/IL-12 showed significant decrease of ALT and AST compared to mice with IL-12 treatment (Fig. 3b ∼ c). At necropsy, vital organs such as the liver, kidney, lung, spleen, and heart were examined for pathological changes (a liver examination is shown in Fig. 3d). The IL-12 treated group exhibited inflammatory cell infiltrates, dilatation of blood sinus, and degeneration in liver tissue. In comparison, the livers of CS-TPP/IL-12 treated mice exhibited inflammatory cell infiltrates in the portal tract, and no other pathological features; this finding led us to conclude that CS-TPP potentially provided a shield from toxicity due to IL-12.

### 3.4. Release of IL-12 from CS-TPP nanoparticles

The association efficiency of nanoparticles was determined by centrifugation, and the amount of free IL-12 in the supernatant was detected by ELISA and compared with the total IL-12 initially added. As shown in Fig. 4a, the loading efficiency was over 28% using the range of weight ratio and IL-12 concentration of 0.1 μg/mL. The pH sensitivity of the nanoparticles was evaluated for the chitosan−TPP formulation with IL-12 loading at concentration of 0.1 μg/mL at pH 6. The nanoparticles were pelleted at $8000 \times g$, which is lower than the force of $20,000 \times g$ required to pellet the smallest nanoparticles, in order to separate the nanoparticles from the free IL-12 without destroying the integrity of the nanoparticles. The in-vitro release profiles of IL-12 (shown in Fig. 4b) exhibited a burst effect within the first hour, followed by a slow release of IL-12 thereafter. However, the IL-12 release profiles were radically different after 6 h, with over 50% of the associated IL-12 released in the dissolution at a pH of 5 or 7, and only 25% of IL-12 released in the dissolution at a pH of 6.

To confirm whether chitosan-TPP/IL-12 nanoparticles remain more highly efficient IL-12 carriers for targeting hepatic tumor metastases in-vivo compared with IL-12, the expression levels of IL-12 were investigated by Western blot. The chitosan-TPP/IL-12 nanoparticles, prepared containing 0.1 μg or 0.2 μg IL-12, were used to treat mice bearing CT26 carcinoma cells daily. As shown in Fig. 4c, IL-12 expression by chitosan-TPP/IL-12 nanoparticles was significantly higher compared to IL-12 and chitosan-TPP alone ($p < 0.05$).

3.5. Intravenous delivery of CS-TPP/IL-12 nanoparticles inhibits CRC liver metastasis

We demonstrated that injection through the intraperitoneal spleen with a dose of 0.2 mL (1×10^6/mL) effectively established an animal model of CRC with liver metastasis as shown in Spl.1. To investigate the immunotherapeutic effect of CS-TPP/IL-12 nanoparticles on CRC hepatic metastasis, mice bearing spleen injections of CT26 carcinoma cells were treated intravenously daily with 0.1 μg or 0.2 μg per mouse of IL-12 loaded in CS-TPP 14 days post-tumor implantation. As hypothesized, systemic delivery of CS-TPP/IL-12 nanoparticles significantly reduced the number of CRC liver metastasis foci compared to the CS-TPP treated group (Fig. 5). Intravenous delivery of IL-12 alone also demonstrated an inhibitory effect on the number of CRC liver metastases. Interestingly, further
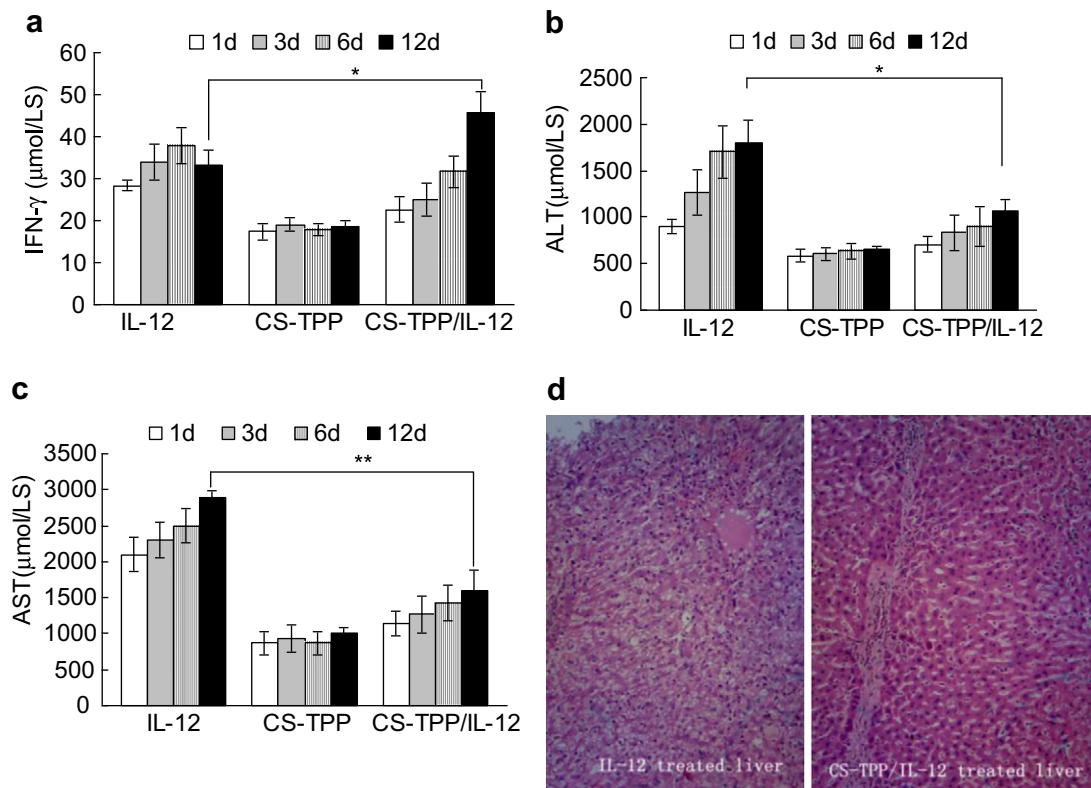
Fig. 3. Chitosan-TPP (200 nm) shielded toxicity of IL-12 during circulation in mice. (a) The plasma level of IFN-γ was measured by ELISA. Plasma was used to measure ALT (b) and AST (c). *Points*, averages of triplicate mice for each time point; *bars*, SDs. *$P < 0.05$, **$P < 0.01$. (d) At 12 days after treatment, H&E staining of mouse livers treated with IL-12 or CS-TPP/IL-12; the IL-12 treated group showed scattered inflammatory cell infiltrates, dilatation of blood sinus, and degeneration in liver tissue. However, CS-TPP/IL-12 treated livers only showed inflammatory cell infiltrates in the portal tract, and no other abnormalities were seen.
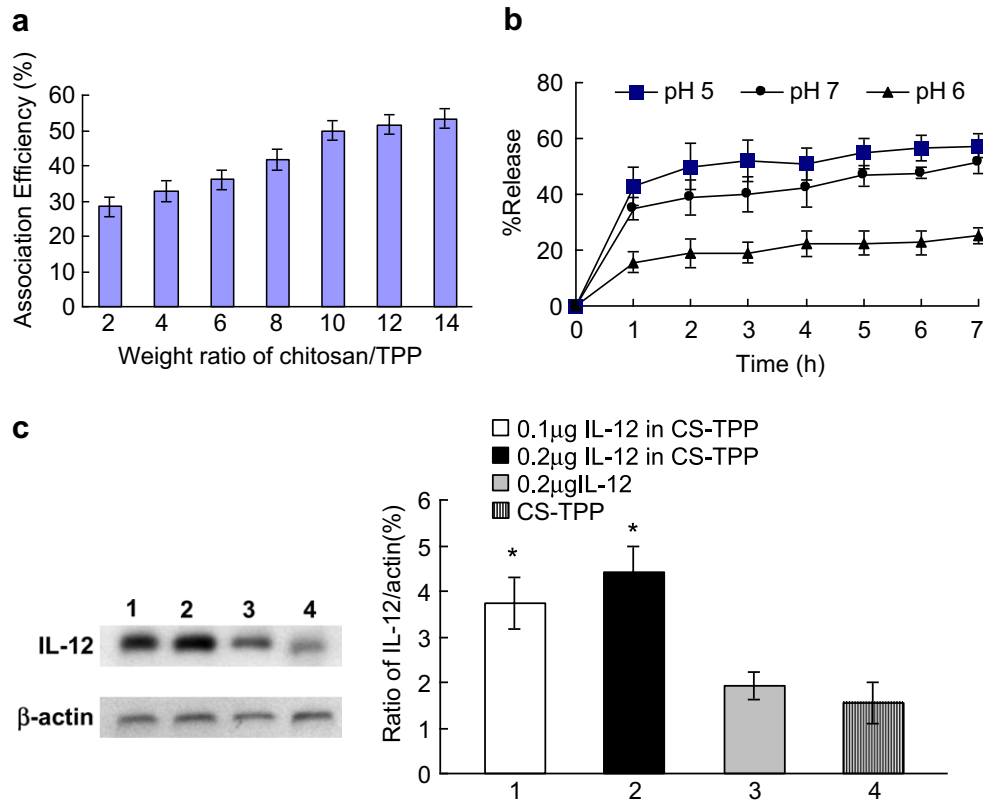
Fig. 4. Release of IL-12 *in-vitro* and *in-vivo*. (a) The AE of IL-12 in nanoparticles (200 nm) prepared at various weight ratios. (b) Release of IL-12 from nanoparticles (200 nm) into various dissolution media at 37 °C. The nanoparticles were prepared with an IL-12 concentration of 1 mg/mL at pH 6. (c) Western blot analysis of IL-12 in tumor tissue of mice bearing CT26 carcinoma cells treated with nanoparticles (200 nm) containing 0.1 μg IL-12 (Line1), 0.2 μg IL-12 (Line2), 0.2 μgIL-12 alone (Line3), and CS-TPP alone (Line4). Data are presented as mean ± SD, n = 3.

examination of the change in hepatic metastasis volume indicated no significant differences between the CS-TPP and the IL-12 treated groups ($p > 0.05$). In addition, our data indicated that mice bearing CT26 carcinoma cells and treated intravenously on a daily basis with 0.2 μg of IL-12 loaded in CS-TPP exhibited significant inhibition of hepatic metastasis volume compared to the group that received 0.1 μg IL-12 loaded nanoparticles.

3.6. Intravenous CS-TPP/IL-12 induced tumor-infiltrating lymphocytes in hepatic metastasis foci

Our data indicated that intravesical CS-TPP/IL-12 could increase local levels of IL-12 in hepatic tumor metastases (Fig. 4c). Therefore, we histologically assessed the liver immune microenvironment. As shown in Fig. 6a, mice treated with IL-12 alone exhibited slight neutrophil infiltration along with a small increase in macrophage recruitment. However, an intravesical CS-TPP/IL-12 induced increase in neutrophil recruitment followed the recruitment of macrophages and lymphocytes after two days of treatment. Immunohistochemical staining revealed that CD8+ T cells, and CD4+ T cells increased significantly with CS-TPP/IL-12 immunotherapy. To further elucidate the cytolytic mechanisms of CS-TPP/IL-12 mediated hepatic tumor regression, we performed a kinetic study of cytolytic activity. MNCs were isolated from animal livers at 2, 4, 8, and 16 days (6 mice/group/time point) after treatment and assayed for direct cytolysis against ^{51}Cr-labeled parental CT26 tumor cells. CS-TPP/IL-12 treatment resulted in significant cytolysis at days 2 and 4, but not in animals treated with IL-12 or CS-TPP alone (Fig. 6b). To further identify the immune effectors, we performed *in-vitro* cell depletion of MNCs isolated from IL-12/

chitosan-TPP nanoparticle treated animal livers at day 3. As shown in Fig. 6c, following depletion of total T cells (Thy1.2), cytolytic activity was only reduced by half, whereas NK cell depletion abolished most of the lytic activity.

4. Discussion

IL-12 based therapies potentiate immunologic memory and have demonstrated remarkable antitumor effects in numerous mouse murine models [31,32]; unfortunately, two deaths that occurred during an IL-12 based clinical phase II study have overshadowed the modest antitumor effects generated by systemically administered IL-12 [15]. At present, few reports have demonstrated successful intravenous administration of IL-12 in preclinical studies, in contrast to local administration of IL-12 [33]. It has been recently reported that local administration of CS-based nanoparticles delivering IL-12 cytokines cured mice bearing orthotopic bladder tumors [23]. Although chitosan is useful in forming a direct complex with IL-12, the properties of chitosan/IL-12 nanoparticles have not been previously elucidated. This has contributed to the lack of uniformity and stability of the complexes due to uncontrolled complex formation. To select optimal nanoparticles capable of prolonged circulation and lower toxicity, we modified CS with TPP and investigated the underlying properties. As Fig. 1 shows, the mean diameter of the nanoparticles increased in certain ranges with an increase of chitosan/TPP weight ratios and incorporation of IL-12 at an increasing concentration, and led to the formation of larger nanoparticles. In addition, the zeta potential of the nanoparticles increased in a certain range depending on the weight ratio of CS to TPP, suggesting a net positive surface charge due to excess
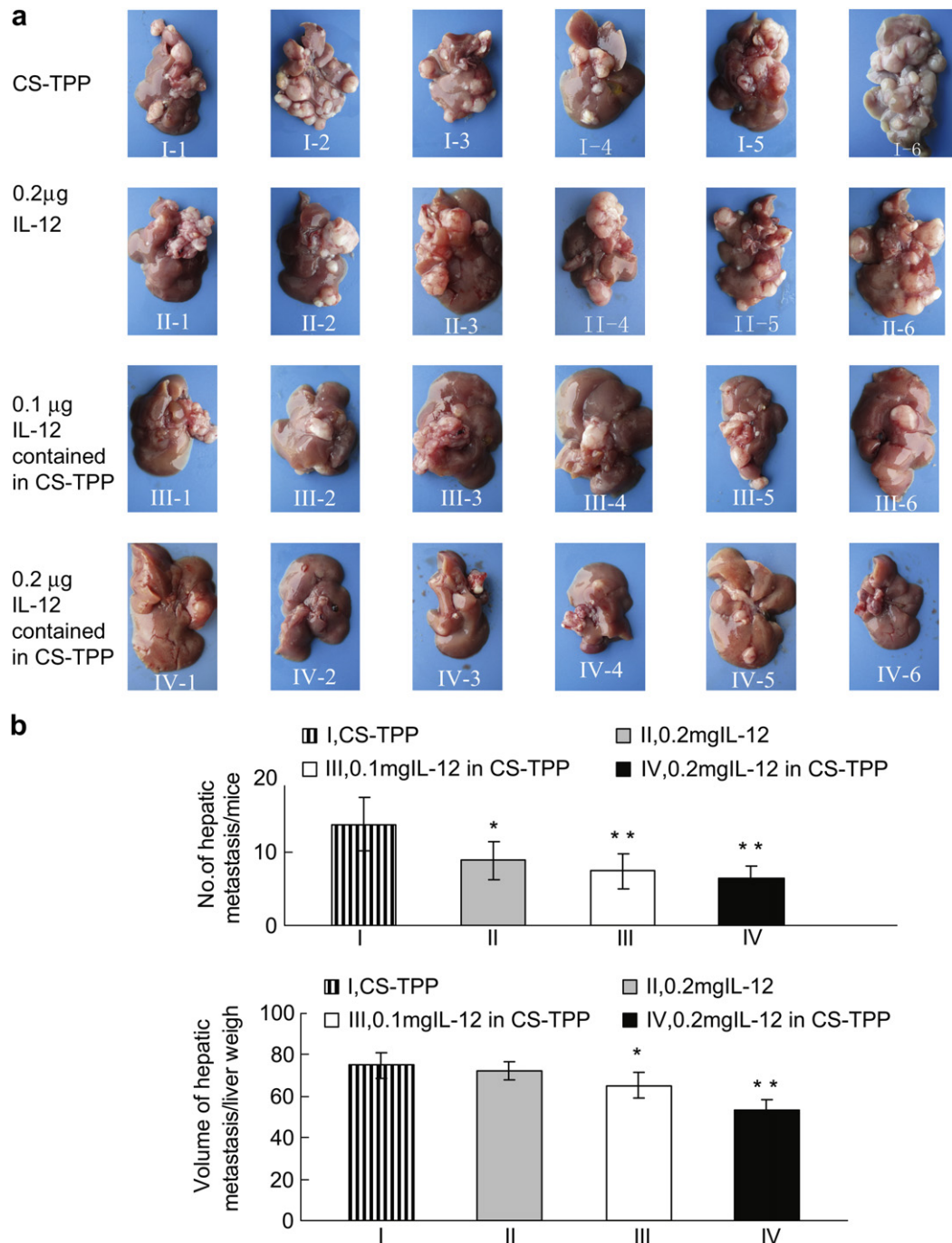
Fig. 5. Prevention of CRC hepatic metastasis by intravenous delivery of CS-TPP/IL-12 (200 nm). BALB/c mice received a spleen injection of CT26 carcinoma cells to induce hepatic metastases. Two weeks later, each mouse was injected intravenously on a daily basis with CS-TPP nanoparticles alone (group I), 0.2 µg IL-12 (group II), 0.1 µg IL-12 contained in CS-TPP (group III), and 0.2 µg IL-12 contained in CS-TPP (group IV). The mice were sacrificed 21 days after tumor challenge, the number of hepatic metastases counted and volume of metastasis measured. (a) Representative photographs of hepatic metastases from each group; (b) Effect of CS-TPP/IL-12 on number of hepatic metastases and volume of hepatic metastasis. Data are presented as mean ± SD, $n = 6$, $*P < 0.05$, $**P < 0.01$, versus CS-TPP group.

chitosan, whereas incorporation of IL-12 at increasing concentrations led to a lower zeta potential. It has been hypothesized that the negatively charged carboxyl in IL-12 competes with TPP in binding the amino groups of chitosan and results in larger sized nanoparticles with lower zeta potentials because of the differing molecular weights between TPP and IL-12; this hypothesis offered a reference for the formulation of a novel delivery system.

We have previously demonstrated the effective enhancement of *in-vitro* transfection efficiency for shRNA with CS-TPP [20]. In this study, to address the lack of information regarding the feasibility of systemic delivery of CS-TPP/IL-12 we investigated the biological features of this protein nano-carrier system *in-vivo*. Because the ability of Balb/c mice to mount a possible immune response to these nanoparticles is compromised due to the developmental defects of the immune organs, the animals were repeatedly injected intravenously with the formulations. Since activation of effector cells such as T lymphocytes and NK cells by IL-12 is accompanied by release of IFN-γ [34], the similar toxicity induced by IL-12 and IFN-γ
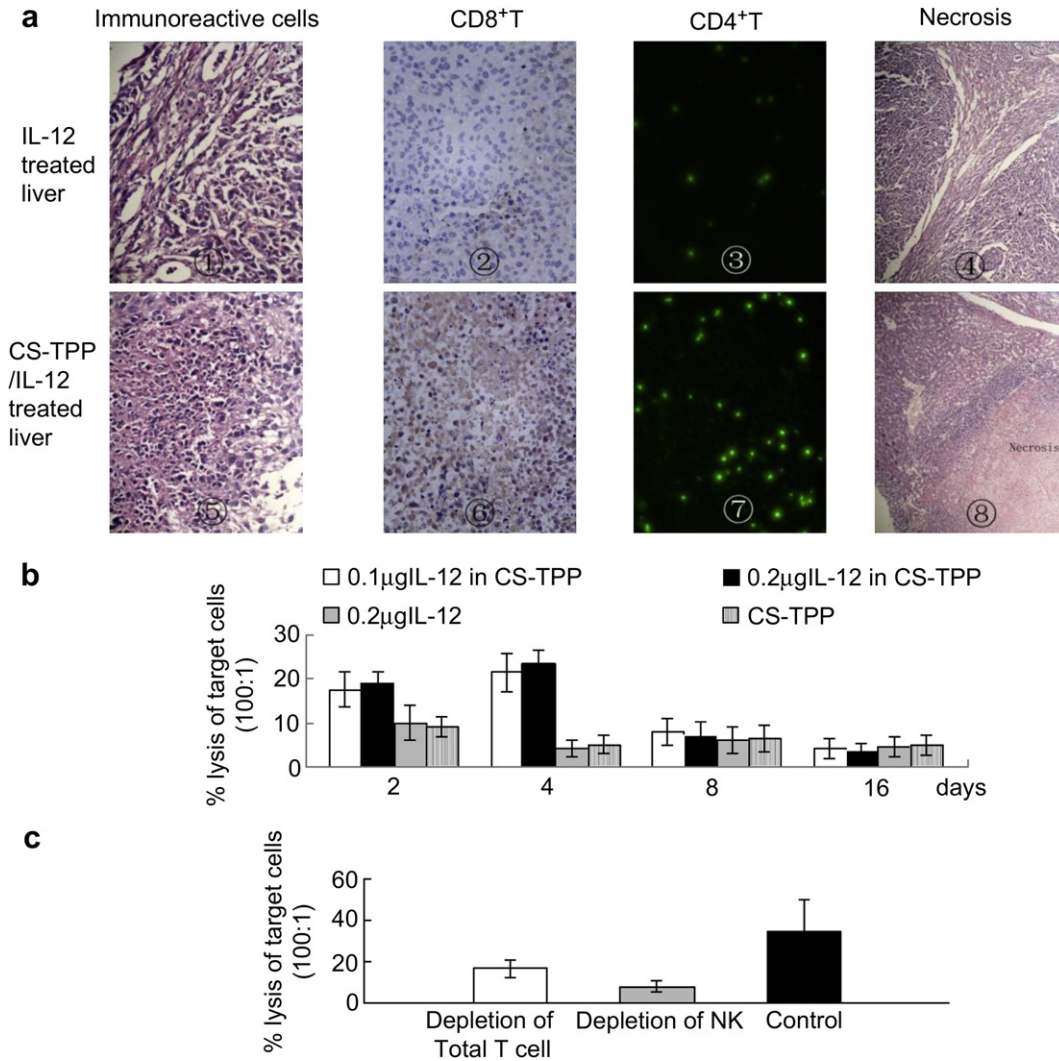
Fig. 6. Evaluation of the liver immune response microenvironment in CS-TPP/IL-12 (200 nm)or IL-12 only treated animals. (a) Hematoxylin–eosin staining of hepatic metastasis immunoreactive cells in mice treated with IL-12(① × 400) and CS-TPP/IL-12(⑤ × 400). Immunohistochemical staining with anti-CD8 antibody of the liver metastatic focus of IL-12-treated (② × 400)(no CD8+-positive cells) and CS-TPP/IL-12 treated mice (⑥ × 400) (scattered CD8+-positive cells). Immunofluorescence staining CD4+ T cells involved in tumor-infiltration in mice treated with IL-12(③ × 400) and CS-TPP/IL-12(⑦ × 400). Hematoxylin-eosin staining of necrotic tumor areas in mice treated with IL-12(④ × 100) and CS-TPP/IL-12(⑧ × 100); (b) Evaluation of the NK cell immune response in liver. MNCs were isolated from animal livers at 2, 4, 8, and 16 days (6 mice/group/time point) after treatment and assayed for direct cytolysis against ^{51}Cr-labeled parental CT26 tumor target. Killing activities were assessed at day 2 and 4 in CS-TPP/IL-12 treated animal livers, but not in animals treated with IL-12 or CS-TPP alone. (c) Identification of the immune effector cells by in-vitro cell depletion. MNCs isolated from CS-TPP/IL-12 nanoparticle treated animal livers at day 3 were depleted by complement lysis of pan-T (Thy1.2) cells, NK(DX5) or complement alone as a control. Total T-cell depletion reduced lytic activity by half, whereas NK cell depletion abolished most of the lytic activity.

treatment [15], and liver enzymes tested are most commonly raised in liver disease, we used the level of IFN-γ, ALT and AST necessary to evaluate the immune response and toxicity in tissue. As shown in Fig. 2, twelve days after treatment with IL-12 the level of IFN-γ decreased gradually; however, the level of IFN-γ in mice treated with CS/IL-12 or CS-TPP/IL-12 continued to increase, even after 12 days. Furthermore, the pathological results exhibited no obvious abnormalities in CS-TPP/IL-12 treated organs. It has been previously demonstrated that phagocytosis by macrophages is strongly enhanced by cationic surface-charged particles [35,36]. We used CS-TPP nanoparticles prepared by the ionic interaction between a negatively charged counter-ion of TPP and a positively charged amino group of CS, and reduced the binding capacity of the nanoparticles with negatively charged opsonins to enable escape from clearance by the monocyte-macrophage system in circulation. Therefore, no obvious hypersensitive toxicity was seen in the mice treated with CS-TPP/IL-12.

Because Kupffer cells are thought to play a major role in clearing particulate materials from systemic circulation [37] and particle size effects intrahepatic distribution [38], it is important to optimize conditions for the preparation of CS-TPP/IL-12. Our results demonstrated that the size of potential liver-targeting nanoparitcles ranges from 100 nm to 200 nm. Although liver endothelial cells are also important scavengers for circulating macromolecules, it has been reported that only small particles are taken up [39]. In addition, the FITC–CS-TPP treated animals exhibited a higher intensity of FI in the liver sections compared to the FITC-CS treated animals, which is potentially related to the positively charged CS nanoparticles, modified by TPP, that improve the stability of CS nanoparticles and allow the encapsulated IL-12 to accumulate in the liver. Furthermore, CS exhibits immmunostimulatory activity by increasing and activating macrophages [40], as shown in Fig. 4c. We demonstrated that nanoparticles mediated a more efficient IL-12 liver targeting in animals bearing CT26 colon cancer cells, which

is potentially due to the large number of new blood vessels in the tumor that recruit macrophages in the liver.

Little is known concerning the mechanisms underlying the digestion of nanoparticles in the liver, although this issue is of utmost importance for the application of liver-targeting nano-technology. In concordance with our findings, we hypothesize that Kupffer cells potentially remove nanoparticles from circulation by endocytosis. During this process, nanoparticles are taken-up by Kupffer cells and directed to lysosomes. The pH-sensitive nano-particles are designed to destabilize in acidic environments such as those found in endocytic vesicles. In this study, the association efficiency and the pH sensitivity of nanoparticles were determined, and the results demonstrated that IL-12 targeting to liver tumor can be achieved by designing pH-sensitive drug delivery system, which disintegrate and release the entrapped drugs in response to at lower pH at tumor site. As we all know that the extracellular pH of the body tissue is maintained around 7.4 in a healthy human. In contrast, the tumor tissue exhibits substantially lower pH values range from 5.7 to 7.8 [41]. This difference in pH between normal tissue and tumors has stimulated many investigators to design pH-sensitive carriers [42]. As shown in Fig. 4b, the IL-12 release profiles were radically different after 6 h in-vitro, with over 50% of the associated IL-12 released in the dissolution at a pH of 5, which suggests that the CS-TPP nanoparticle formulation with IL-12 loaded at concentration of 0.1 μg/mL at pH 6 exhibits a suitable pH sensitivity; this was confirmed by Western blot analysis of IL-12 expression.

We tested effect of intravenous delivery with CS-TPP/IL-12 nanoparticles on CRC liver metastases. Firstly, we selected a suit-able CRC liver metastasis study model by way of intraperitoneal spleen transplant with a dose of 0.2 mL (1×10^6/mL) (Spl.1). Three weeks later, mice bearing CT26 carcinoma cells were treated intravenously on a daily basis with CS-TPP/IL-12 for 14 days post tumor implantation. The systemic delivery of CS-TPP/IL-12 nano-particles significantly reduced the number of CRC liver metastasis foci in a dose-dependent manner compared to the CS treated group. To elucidate the underlying mechanism of inhibition of CRC hepatic metastases by CS-TPP/IL-12 nanoparticles, the immune response microenvironment was analyzed. As we hypothesized, systemic delivery of CS-TPP/IL-12 induced infiltration of microphages and T cells, which are likely effector cells mediating tumor metastasis inhibition during CS-TPP/IL-12 immunotherapy. It would be of interest to identify the effector cells involved in CS-TPP/IL-12 immunotherapy, as these cells represent the major effector cells for the IL-12-activated innate immune response [43]. Our data showed that cytolytic activity was only reduced by half upon total depletion of T (Thy1.2) cells, whereas NK cell depletion abolished most of the lytic activity. These results indicate that NK cells and some NKT cells are involved in the antitumor response.

5. Conclusion

We designed CS modified with TPP as an IL-12 protein carrier. Our results indicate that we can modulate their biodistribution and release rate by adjusting the formulation parameters. Intravenous delivery of the CS-TPP/IL-12 complex inhibited CRC hepatic metastasis by inducing infiltration of NK cells and some T cells in the liver. Therefore, CS-based nanoparticles exhibit the potential to comprise a safe liver-targeting cytokine delivery system, and the ensuing accumulation of IL-12 in the liver can trigger liver resident antitumor immunity.

Competing interest

None declared.

Appendix. Supplementary material

Supplementary material associated with this article can be found, in the online version, at doi:10.1016/j.biomaterials.2012.02.014.

References

[1] Geoghegan JG, Scheele J. Treatment of colorectal liver metastases. Br J Surg 1999;86:158–69.
[2] Barugel ME, Vargas C, Krygier Waltier G. Metastatic colorectal cancer: recent advances in its clinical management. Expert Rev Anticancer Ther 2009;9: 1829–47.
[3] Coffey JC, Wang JH, Smith MJ, Bouchier-Hayes D, Cotter TG, Redmond HP. Excisional surgery for cancer cure: therapy at a cost. Lancet Oncol 2003;4: 760–8.
[4] van der Bij GJ, Oosterling SJ, Bogels M, Bhoelan F, Fluitsma DM, Beelen RH, et al. Blocking alpha2 integrins on rat CC531s colon carcinoma cells prevents operation-induced augmentation of liver metastases outgrowth. Hepatology 2008;47:532–43.
[5] Oosterling SJ, van der Bij GJ, Bogels M, ten Raa S, Post JA, Meijer GA, et al. Anti-beta1 integrin antibody reduces surgery-induced adhesion of colon carcinoma cells to traumatized peritoneal surfaces. Ann Surg 2008;247:85–94.
[6] Cleary JM, Tanabe KT, Lauwers GY, Zhu AX. Hepatic toxicities associated with the use of preoperative systemic therapy in patients with metastatic colo-rectal adenocarcinoma to the liver. Oncologist 2009;14:1095–105.
[7] Eng C. Toxic effects and their management: daily clinical challenges in the treatment of colorectal cancer. Nat Rev Clin Oncol 2009;6:207–18.
[8] Grimm M, Gasser M, Bueter M, Strehl J, Wang J, Nichiporuk E, et al. Evaluation of immunological escape mechanisms in a mouse model of colorectal liver metastases. BMC Cancer 2010;10:82.
[9] Pages F, Kirilovsky A, Mlecnik B, Asslaber M, Tosolini M, Bindea G, et al. In situ cytotoxic and memory T cells predict outcome in patients with early-stage colorectal cancer. J Clin Oncol 2009;27:5944–51.
[10] Weiner LM, Surana R, Wang S. Monoclonal antibodies: versatile platforms for cancer immunotherapy. Nat Rev Immunol 2010;10:317–27.
[11] van der Bij GJ, Bögels M, Otten MA, Oosterling SJ, Kuppen PJ, Meijer S, et al. Experimentally induced liver metastases from colorectal cancer can be pre-vented by mononuclear phagocyte-mediated monoclonal antibody therapy. J Hepatol 2010;53:677–85.
[12] Rivoltini L, Mazzaferro V. Exploiting liver immunity for the prevention of hepatic metastases. J Hepatol 2010;53:596–6.
[13] Del Vecchio M, Bajetta E, Canova S, Lotze MT, Wesa A, Parmiani G, et al. Interleukin-12: biological properties and clinical application. Clin Cancer Res 2007;13:4677–85.
[14] Cheever MA. Twelve immunotherapy drugs that could cure cancers. Immunol Rev 2008;222:357–68.
[15] Leonard JP, Sherman ML, Fisher GL, Buchanan LJ, Larsen G, Atkins MB, et al. Effects of single-dose interleukin-12 exposure on interleukin-12-associated toxicity and interferon-gamma production. Blood 1997;90:2541–8.
[16] Salem ML, Gillanders WE, Kadima AN, El-Naggar S, Rubinstein MP, Demcheva M, et al. Review: novel nonviral delivery approaches for interleukin-12 protein and gene systems: curbing toxicity and enhancing adjuvant activity. J Interferon Cytokine Res 2006;26:593–608.
[17] Cohen J. IL-12 deaths: explanation and a puzzle. Science 1995;270:908.
[18] Dranoff G. The use of gene transfer in cancer immunotherapy. Forum (Genova) 1998;8:357–64.
[19] Colombo MP, Vagliani M, Spreafico F, Parenza M, Chiodoni C, Melani C, et al. Amount of interleukin 12 available at the tumor site is critical for tumor regression. Cancer Res 1996;56:2531–4.
[20] Wang SL, Yao HH, Guo LL, Dong L, Li SG, Gu YP, et al. Selection of optimal sites for TGFB1 gene silencing by chitosan-TPP nanoparticle-mediated delivery of shRNA. Cancer Genet Cytogenet 2009;190:8–14.
[21] Wang SL, Yao HH, Qin ZH. Strategies for short hairpin RNA delivery in cancer gene therapy. Expert Opin Biol Ther 2009;9:1357–68.
[22] Kim TH, Jin H, Kim HW, Cho MH, Cho CS. Mannosylated chitosan nanoparticle-based cytokine gene therapy suppressed cancer growth in BALB/c mice bearing CT-26 carcinoma cells. Mol Cancer Ther 2006;5:1723–32.
[23] Zaharoff DA, Hoffman BS, Hooper HB, Benjamin Jr CJ, Khurana KK, Hance KW, et al. Intravesical immunotherapy of superficial bladder cancer with chitosan/interleukin-12. Cancer Res 2009;69:6192–9.
[24] Kato Y, Onishi H, Machida Y. Biological characteristics of lactosaminated N-succinyl-chitosan as a liver-specific drug carrier in mice. J Control Release 2001;70:295–307.

[25] Wu DQ, Lu B, Chang C, Chen CS, Wang T, Zhang YY, et al. Galactosylated fluorescent labeled micelles as a liver targeting drug carrier. Biomaterials 2009;30:1363—71.

[26] Lopez-Leon T, Carvalho EL, Seijo B, Ortega-Vinuesa JL, Bastos-Gonzalez D. Physicochemical characterization of chitosan nanoparticles: electrokinetic and stability behavior. J Colloid Interface Sci 2005;283:344—51.

[27] Chow LW, Loo WT, Yuen KY, Cheng C. The study of cytokine dynamics at the operation site after mastectomy. Wound Repair Regen 2003;11:326—30.

[28] Di Vita G, Patti R, D'Agostino P, Caruso G, Arcara M, Buscemi S, et al. Cytokines and growth factors in wound drainage fluid from patients undergoing incisional hernia repair. Wound Repair Regen 2006;14:259—64.

[29] Pham-Nguyen KB, Yang W, Saxena R, Thung SN, Woo SL, Chen SH. Role of NK and T cells in IL-12-induced anti-tumor response against hepatic colon carcinoma. Int J Cancer 1999;81:813—9.

[30] Gupta AK, Gupta M. Synthesis and surface engineering of iron oxide nanoparticles for biomedical applications. Biomaterials 2005;26: 3995—4021.

[31] Lo CH, Chang CM, Tang SW, Pan WY, Fang CC, Chen Y, et al. Differential antitumor effect of interleukin-12 family cytokines on orthotopic hepatocellular carcinoma. J Gene Med 2010;12:423—34.

[32] Colombo MP, Trinchieri G. Interleukin-12 in anti-tumor immunity and immunotherapy. Cytokine Growth Factor Rev 2002;13:155—68.

[33] Weiss GR, O'Donnell MA, Loughlin K, Zonno K, Laliberte RJ, Sherman ML. Phase 1 study of the intravesical administration of recombinant human interleukin-12 in patients with recurrent superficial transitional cell carcinoma of the bladder. J Immunother 2003;26:343—8.

[34] Gately MK, Warrier RR, Honasoge S, Carvajal DM, Faherty DA, Connaughton SE, et al. Administration of recombinant IL-12 to normal mice enhances cytolytic lymphocyte activity and induces production of IFN-gamma in vivo. Int Immunol 1994;6:157—67.

[35] Thiele L, Rothen-Rutishauser B, Jilek S, Wunderli-Allenspach H, Merkle HP, Walter E. Evaluation of particle uptake in human blood monocyte-derived cells in vitro. Does phagocytosis activity of dendritic cells measure up with macrophages? J Control Release 2001;76:59—71.

[36] Foged C, Brodin B, Frokjaer S, Sundblad A. Particle size and surface charge affect particle uptake by human dendritic cells in an in vitro model. Int J Pharm 2005;298:315—22.

[37] Sadauskas E, Wallin H, Stoltenberg M, Vogel U, Doering P, Larsen A, et al. Kupffer cells are central in the removal of nanoparticles from the organism. Part Fibre Toxicol 2007;4:10.

[38] Ogawara K, Yoshida M, Higaki K, Kimura T, Shiraishi K, Nishikawa M, et al. Hepatic uptake of polystyrene microspheres in rats: effect of particle size on intrahepatic distribution. J Control Release 1999;59:15—22.

[39] Lenaerts V, Nagelkerke JF, Van Berkel TJ, Couvreur P, Grislain L, Roland M, et al. In vivo uptake of polyisobutyl cyanoacrylate nanoparticles by rat liver Kupffer, endothelial, and parenchymal cells. J Pharm Sci 1984;73:980—2.

[40] Seferian PG, Martinez ML. Immune stimulating activity of two new chitosan containing adjuvant formulations. Vaccine 2000;19:661—8.

[41] Dellian M, Helmlinger G, Yuan F, Jain RK. Fluorescence ratio imaging of interstitial pH in solid tumours: effect of glucose on spatial and temporal gradients. Br J Cancer 1996;74:1206—15.

[42] Lee ES, Gao Z, Bae YH. Recent progress in tumor pH targeting nanotechnology. J Control Release 2008;132:164—70.

[43] Trinchieri G. Interleukin-12: a proinflammatory cytokine with immunoregulatory functions that bridge innate resistance and antigen-specific adaptive immunity. Annu Rev Immunol 1995;13:251—76.